Supplementary Information for "Future changes in South Asian summer monsoon circulation under global warming: Role of the Tibetan Plateau latent heating"

Haolin Luo[1], Ziqian Wang[1, 2, *], Chao He[3], Deliang Chen[4], and Song Yang[1, 2, *]

[1] School of Atmospheric Sciences, Sun Yat-sen University and Southern Marine Science and Engineering Guangdong Laboratory (Zhuhai), Zhuhai, China

[2] Guangdong Province Key Laboratory for Climate Change and Natural Disaster Studies, Sun Yat-sen University, Zhuhai, China

[3] Institute for Environmental and Climate Research, Jinan University, Guangzhou, China

[4] Regional Climate Group, Department of Earth Sciences, University of Gothenburg, Gothenburg, Sweden

*Corresponding authors:

Ziqian Wang, wangziq5@mail.sysu.edu.nc

Song Yang, yangsong3@mail.sysu.edu.cn

Contents of this file

Supplementary Figures

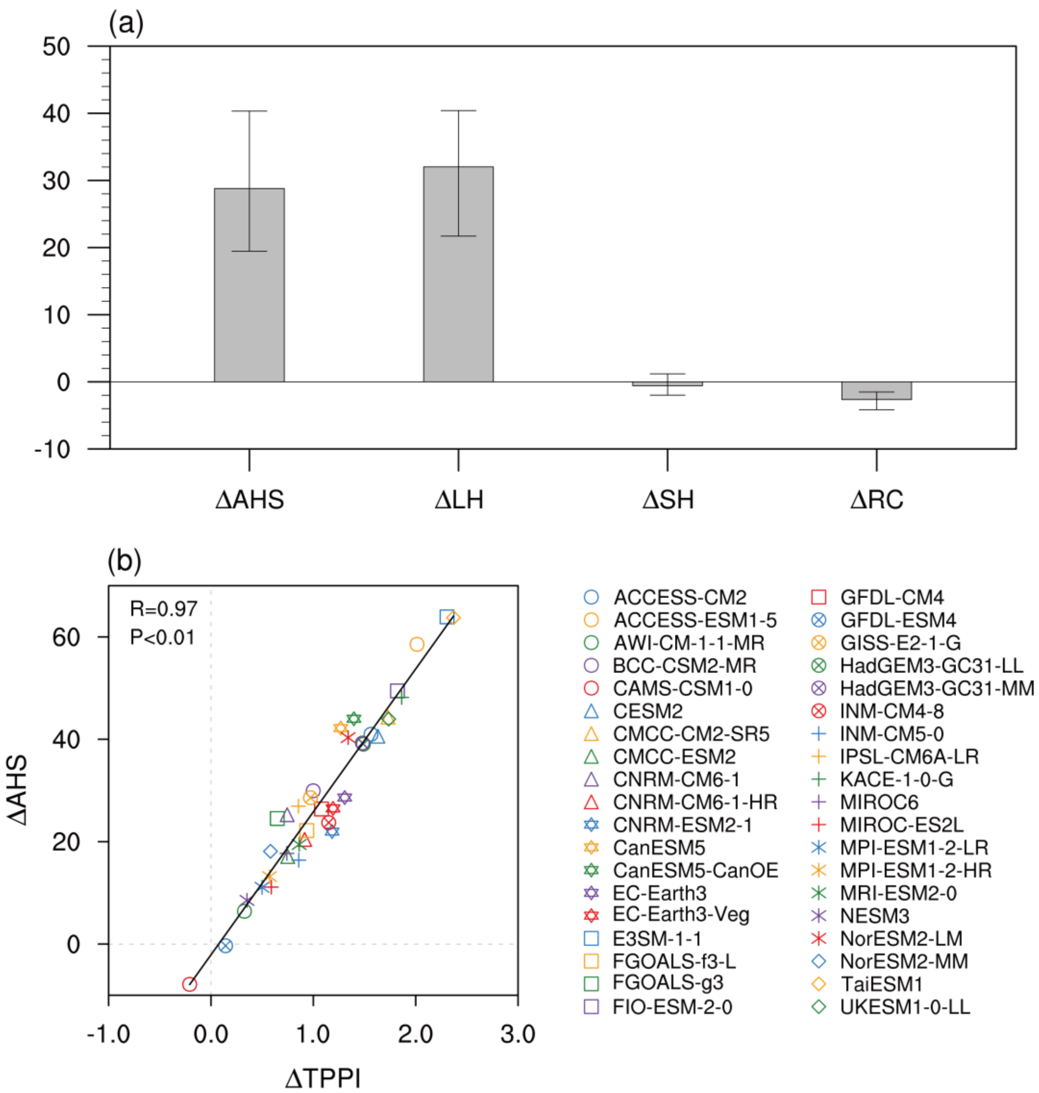

Supplementary Figure 1. (a) Projected changes in atmospheric heat source (AHS) and its different components as latent heating (LH), sensible heating (SH) and radiation cooling (RC) over the TP (75°E–102°E, 25°N–37°N). (b) Inter-model relationship between the projected changes in AHS (W m^{-2}) over the TP and TPI (mm day^{-1}) during 2050–2099 under the SSP5-8.5 scenario, relative to 1965–2014. The whisker in (a) denotes the inter-model spread shown by the 30th and 70th percentiles among 38 models.

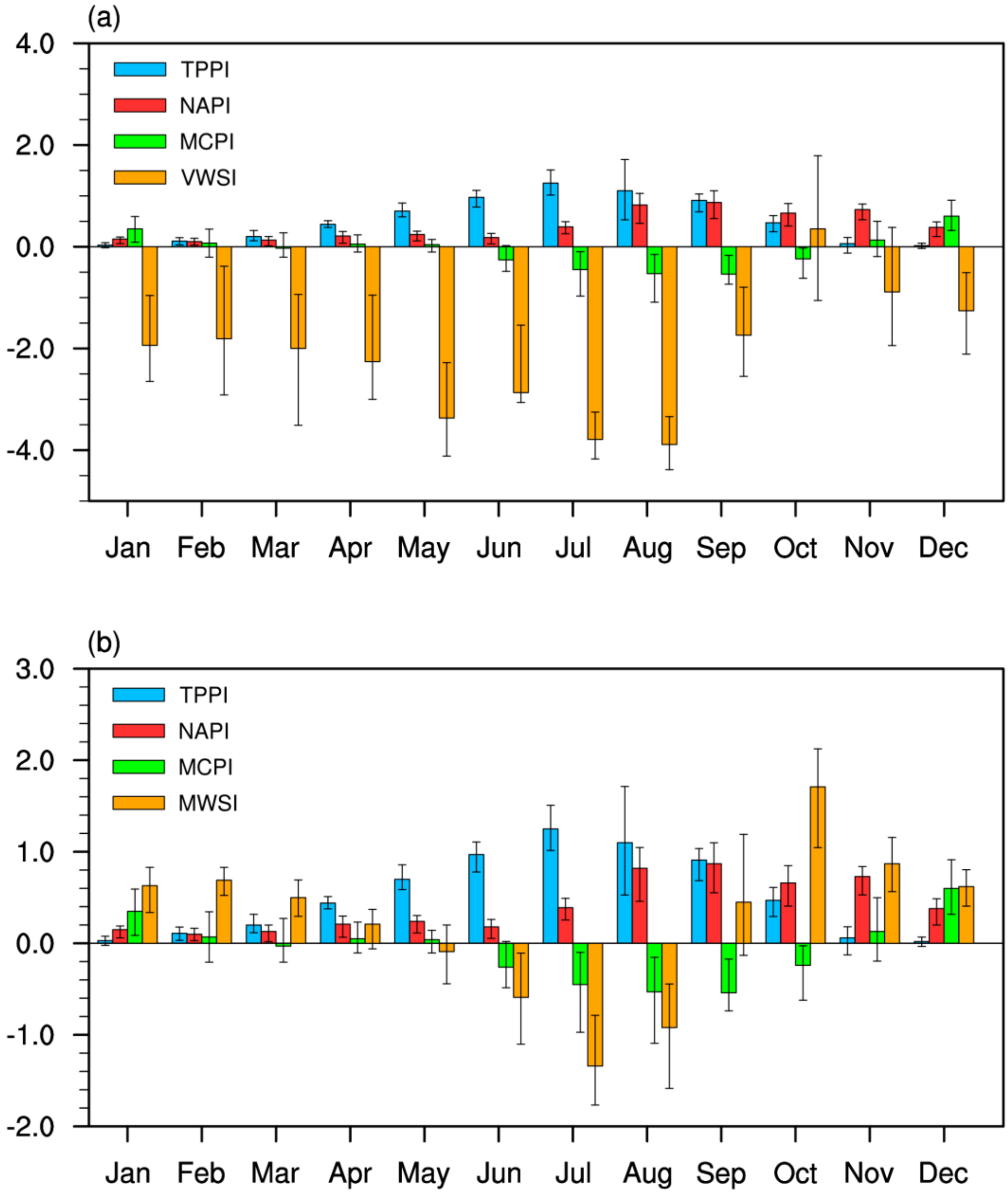

Supplementary Figure 2. Same as Fig. 2, but for the other two SASM circulation indices: (**a**) VWSI (**b**) MWSI.

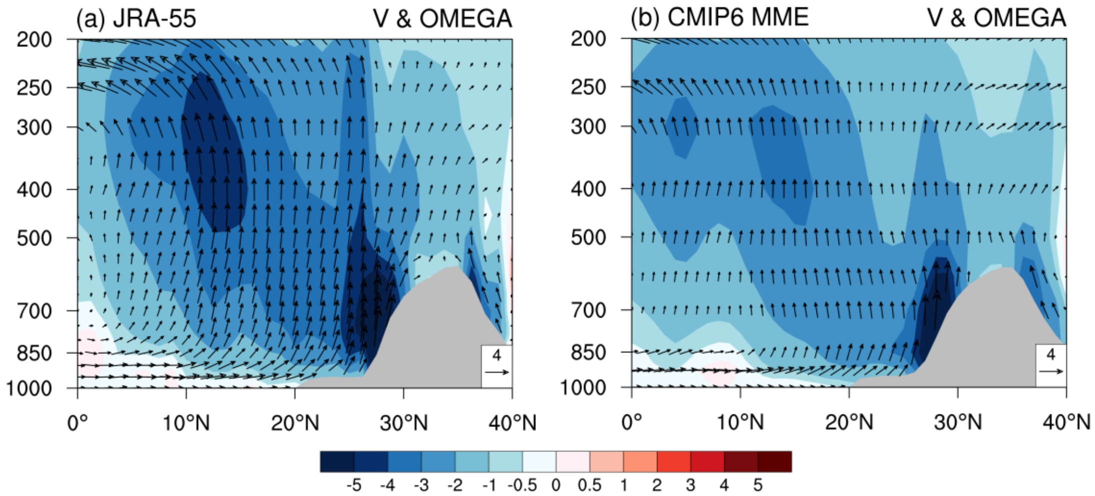

Supplementary Figure 3. Climatological summer vertical velocity (shading, 50 Pa s^{-1}) and meridional circulation (vectors, units of meridional wind and vertical velocity are m s^{-1} and -50 Pa s^{-1}, respectively) averaged over 75°–100°E during 1965–2014 for **a** JRA-55 and **b** CMIP6 MME.

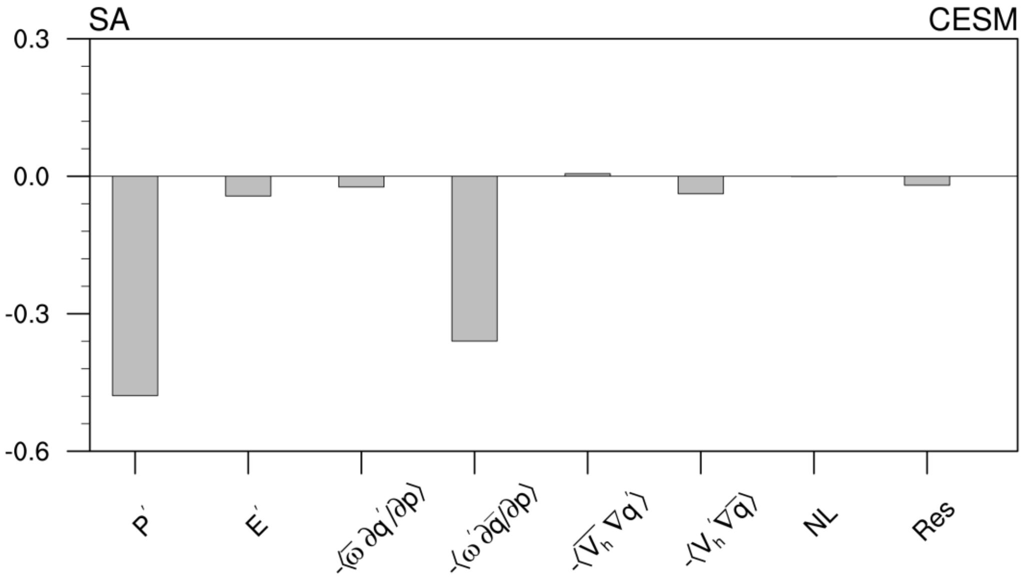

Supplementary Figure 4. Same as Fig. 6b, but for the difference between the results from experiment **TPheat** and experiment **Con**.

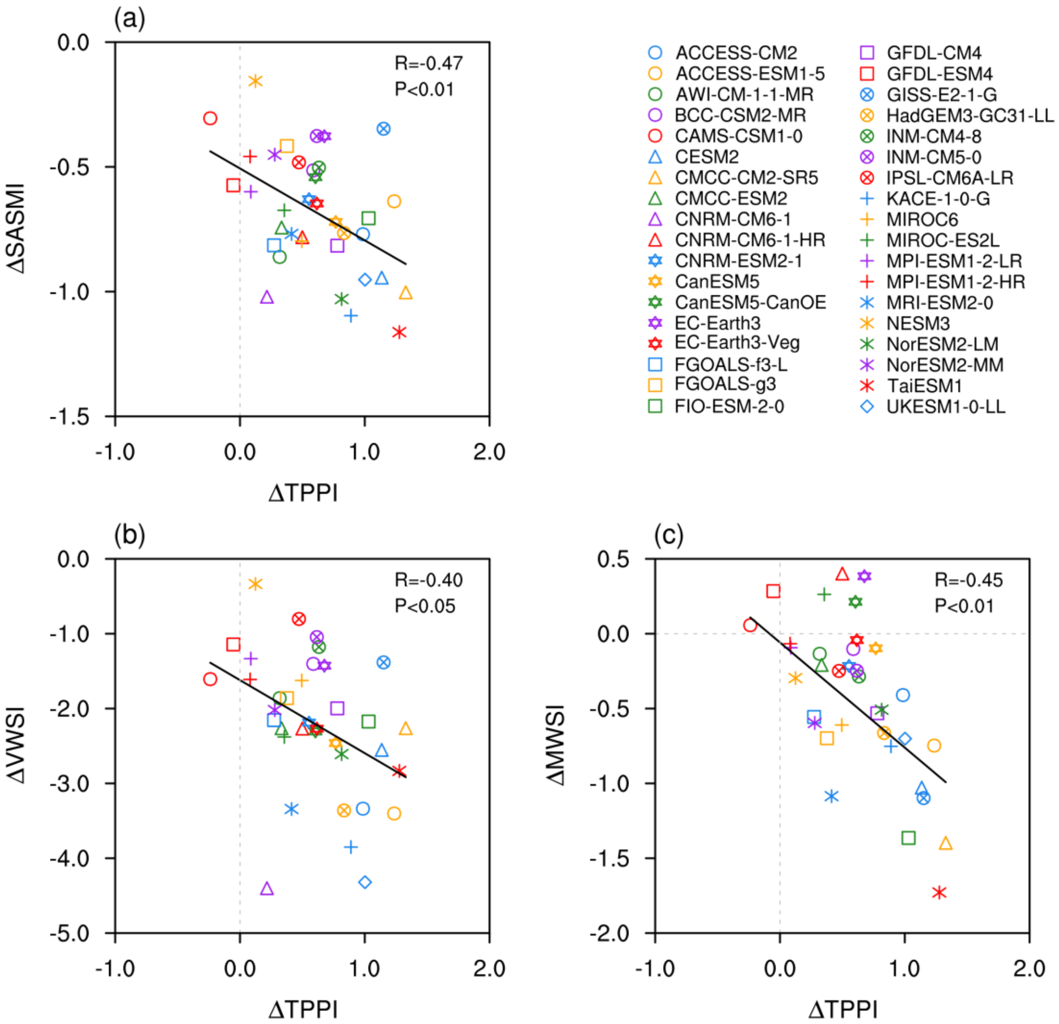

Supplementary Figure 5. Same as Fig. 3, but for 36 available models from SSP2-4.5.

Supplementary Table

No.	Model	Institution/Country	Resolution (lon × lat)
1	ACCESS-CM2	CSIRO-BOM/Australia	192 × 144
2	ACCESS-ESM1-5	CSIRO-BOM/Australia	192 × 145
3	AWI-CM-1-1-MR	AWI/Germany	384 × 192
4	BCC-CSM2-MR	BCC-CMA/China	320 × 160
5	CAMS-CSM1-0	CAMS/China	320 × 160
6	CESM2	NCAR/USA	288 × 192
7	CMCC-CM2-SR5	CMCC/Italy	288 × 192
8	CMCC-ESM2	CMCC/Italy	288 × 192
9	CNRM-CM6-1	CNRM-CERFACS/France	256 × 128
10	CNRM-CM6-1-HR	CNRM-CERFACS/France	720 × 360
11	CNRM-ESM2-1	CNRM-CERFACS/France	256 × 128
12	CanESM5	CCCMA/Canada	128 × 64
13	CanESM5-CanOE	CCCMA/Canada	128 × 64
14	EC-Earth3	EC-Earth-Consortium	512 × 256
15	EC-Earth3-Veg	EC-Earth-Consortium	512 × 256
16	E3SM-1-1	LLNL-DOE/USA	360 × 180
17	FGOALS-f3-L	LASG-IAP/China	288 × 180
18	FGOALS-g3	LASG-IAP/China	180 × 80
19	FIO-ESM-2-0	FIO-RONM/China	288 × 192
20	GFDL-CM4	GFDL-NOAA/USA	288 × 180

21	GFDL-ESM4	GFDL-NOAA/USA	288 × 180
22	GISS-E2-1-G	GISS-NASA/USA	144 × 90
23	HadGEM3-GC31-LL	MOHC/UK	192 × 144
24	HadGEM3-GC31-MM	MOHC/UK	432 × 324
25	INM-CM4-8	INM/Russia	180 × 120
26	INM-CM5-0	INM/Russia	180 × 120
27	IPSL-CM6A-LR	IPSL/France	144 × 143
28	KACE-1-0-G	NIMS-KMA/Korea	192 × 144
29	MIROC6	MIROC/Japan	256 × 128
30	MIROC-ES2L	MIROC/Japan	128 × 64
31	MPI-ESM1-2-LR	MPI/Germany	192 × 96
32	MPI-ESM1-2-HR	MPI/Germany	384 × 192
33	MRI-ESM2-0	MRI/Japan	320 × 160
34	NESM3	NUIST/China	192 × 96
35	NorESM2-LM	NCC/Norway	144 × 96
36	NorESM2-MM	NCC/Norway	288 × 192
37	TaiESM1	RCEC-AS/China	288 × 192
38	UKESM1-0-LL	MOHC/UK	192 × 144

Supplementary Table 1. Summary of the CMIP6 models used in this study.

Supplementary Methods

The atmospheric data in Supplementary Fig. 3a are derived from the Japanese 55-year Reanalysis (JRA-55)[1] by the Japan Meteorological Agency (JMA) with a horizontal resolution of 1.25°×1.25°.

The latent heating (LH), radiation cooling (RC) and atmospheric heat source (AHS) are calculated as follows[2]:

$$\Delta \mathrm{LH} = \Delta \mathrm{Pr} \times \mathrm{L_w} \tag{1}$$

$$\Delta \mathrm{RC} = \Delta\left\{\left(S_\infty^{\downarrow} - S_\infty^{\uparrow}\right) - \left(S_0^{\downarrow} - S_0^{\uparrow}\right) - \left(F_0^{\downarrow} - F_0^{\uparrow}\right) - F_\infty\right\} \tag{2}$$

$$\Delta \mathrm{AHS} = \Delta \mathrm{LH} + \Delta \mathrm{SH} + \Delta \mathrm{RC} \tag{3}$$

where Pr is the precipitation rate, Lw is the condensation heat coefficient, *S* and *F* denote shortwave and longwave radiation fluxes, respectively, the superscripts ↓ and ↑ represent downward and upward transport of the radiation flux, respectively, the subscripts ∞ and 0 denote the net radiation values measured at the top of the atmosphere and at the surface, respectively. The triangle Δ denotes the difference between 2050–2099 and 1965–2014.

Supplementary References

1. Kobayashi, S. et al. The JRA-55 Reanalysis: General specifications and basic characteristics. *J. Meteor. Soc. Japan* **93**, 5–48 (2015).

2. Duan, A. et al. Atmospheric heat source/sink dataset over the Tibetan Plateau based on satellite and routine meteorological observations. *Big Earth Data* **2**, 179–189 (2018).